G&G Lab Notes

Editors
Thomas M. Moses | Shane F. McClure

DIAMOND

Fracture-Filled Diamond with "Rainbow" Flash Effect

A loose diamond submitted for a diamond grading report is evaluated and given a grade on a scale relative to each value factor. Clarity, defined as a diamond's relative freedom from inclusions or blemishes, is graded on a scale of Flawless (least included) to I_3 (most included). The most common inclusions in diamond are crystals, which are contained entirely within the stone, and fractures—also known as feathers—which are surface reaching. Various clarity treatments exist to mask or remove undesirable inclusions because high-clarity diamonds are considered more valuable. Some diamond clarity treatments are permanent, while others are not and may change drastically in appearance with time or improper care. For this reason, GIA does not issue grading reports for diamonds that have been treated with unstable, non-permanent treatments. Acceptable treatments such as laser drilling and internal laser drilling are always clearly disclosed on grading reports.

One such unstable treatment is fracture filling. Large, deep fractures in a diamond will often appear white or reflective due to the difference in the refractive index of the diamond and the air within the fracture. In an effort to disguise this, a substance with a refractive index similar to diamond's, such as highly refractive lead glass, is introduced into surface-reaching fractures to reduce the interference of air (figure 1). Several telltale signs, such as the flash effect, typically reveal the presence of a filled fracture. The classic flash effect displays a vivid pink color in darkfield illumination and a complementary green color in brightfield illumination (figure 2). In a different orientation in brightfield lighting, a filled fracture can also appear bright blue.

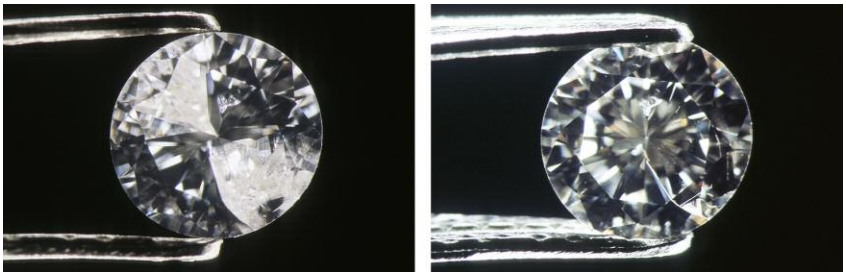

Figure 1. Large fractures in this diamond are exposed in high relief before treatment (left). After the fractures are filled, the same stone has a much improved apparent clarity (right).

A 1.21 ct near-colorless square modified brilliant diamond was recently submitted to GIA's Carlsbad laboratory for a diamond grading report (figure 3). It was rejected for grading after examination revealed a large filled fracture. Interestingly, the flash effect looked noticeably different from the classic appearance described

Figure 2. The classic flash effect appearance: a pink flash in darkfield lighting (left) and a complementary green flash in brightfield lighting (right).

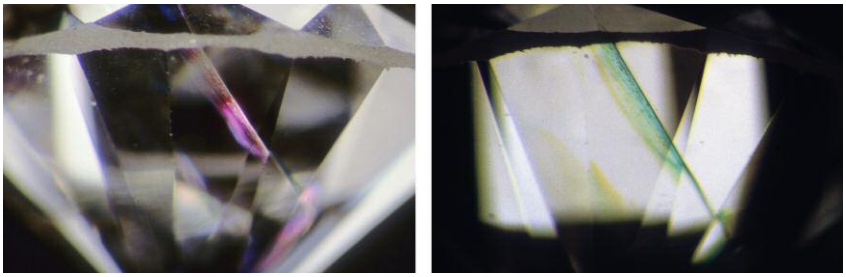

Editors' note: All items were written by staff members of GIA laboratories.

Gems & Gemology, Vol. 54, No. 1, pp. 56–64.

Figure 3. A face-up view of the near-colorless 1.21 ct fracture-filled square modified brilliant cut.

above. Rather than flashing a single color in darkfield lighting and a single complementary color in brightfield lighting, this filled fracture flashed multiple colors in darkfield and multiple complementary colors in brightfield (figure 4). The unusual effect may be due to a difference in ingredients used to manufacture the filling material. To the untrained eye, it could easily be mistaken for the natural iridescence very commonly seen in unfilled fractures. However, such iridescence typically appears when the viewing angle is nearly perpendicular to the fracture, while the flash

Figure 5. In addition to a "rainbow" flash effect, this filled fracture displays a dendritic pattern (and its mirror reflection) at the opening of the fracture. This pattern occurs as a result of incomplete fracture filling. Field of view 1.83 mm.

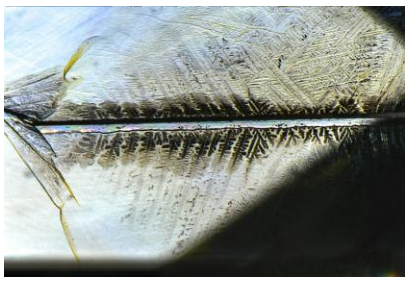

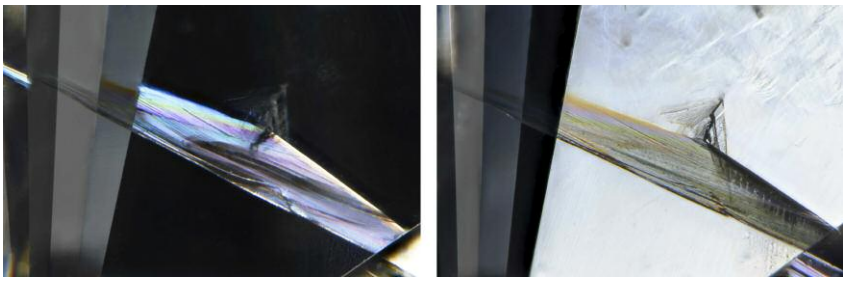

Figure 4. When viewed nearly parallel to the plane of the fracture, this filled fracture exhibits a multicolored "rainbow" flash effect in both darkfield illumination (left) and brightfield illumination (right), as opposed to a classic single-color flash effect. Field of view 2.21 mm.

effect is most visible when the viewing angle is nearly parallel to the plane of the fracture. In addition to the "rainbow" flash effect, this filled fracture showed a dendritic pattern at the fracture opening that is caused by air pockets in the filling substance (figure 5). This pattern is characteristic of incomplete fracture filling (J.I. Koivula, *The MicroWorld of Diamonds*, Gemworld International, Inc., Northbrook, Illinois, 2000, pp. 106–108) and provides further evidence of the treatment.

Hollie McBride

HPHT-Processed Diamond Fraudulently Represented as Untreated

The Hong Kong lab recently encountered another instance of fraud: A natural but HPHT-treated round brilliant diamond (figure 6, left) weighing more than 6 carats submitted for verification service was found to be inconsistent with the claimed GIA report issued a few months prior for an untreated diamond. Moreover, the GIA report number and another inscription on the girdle, both supposedly laser-inscribed by GIA (figure 6, right), looked convincing but were also found to be fraudulent.

The HPHT-processed round brilliant was believed to have been carefully selected to match the original diamond—its color grade (F) matched, and only minor differences were observed in carat weight and measurements. The HPHT-processed diamond weighed 6.30402 ct and measured 11.73–11.82 × 7.32 mm, whereas the original one weighed slightly less (6.30216 ct), and measured 11.72–11.83 × 7.32 mm. Furthermore, the IF

Figure 6. This 6.30 ct round brilliant diamond (left) with a fraudulent inscription of a GIA report number (right) from a similar-looking diamond was confirmed to have been HPHT processed for color improvement.

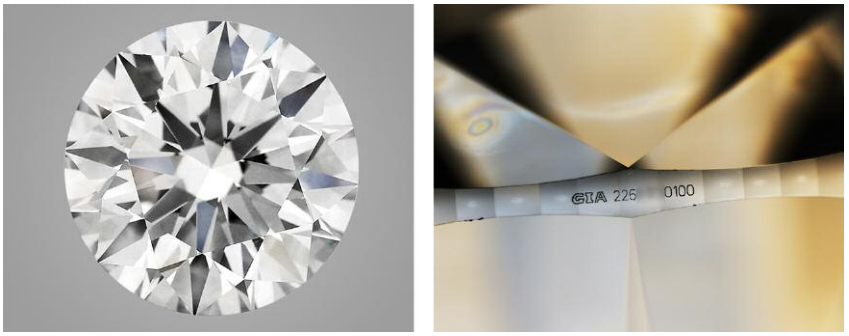

clarity of the HPHT-treated stone was an improvement over the VVS_1 clarity of the natural stone.

Despite all the efforts put into those convincing features and measurements, spectroscopic testing easily revealed the stone's true identity. Infrared absorption spectroscopy showed the HPHT-processed diamond was type IIa, but the original diamond was type Ia. Photoluminescence (PL) spectra were collected at liquid nitrogen temperature with various excitation wavelengths. The slight reversal in the ratio between the 575 and 637 nm peaks (NV centers), together with other spectroscopic features, confirmed the stone had gone through an HPHT treatment process for color improvement. A strain pattern observed under cross-polarized light ruled out the possibility of a synthetic diamond.

This case should raise awareness among the industry and the public that, although rarely encountered in larger stones, this kind of fraud does exist. Verification services at GIA confirm that an item is exactly the same as the one described on a previous report and has not been recut or treated—or, as in this case, replaced with a similar-looking stone. This provides a simple way to check for any type of fraudulent activity if there is doubt about the origin of a diamond.

Billie Law

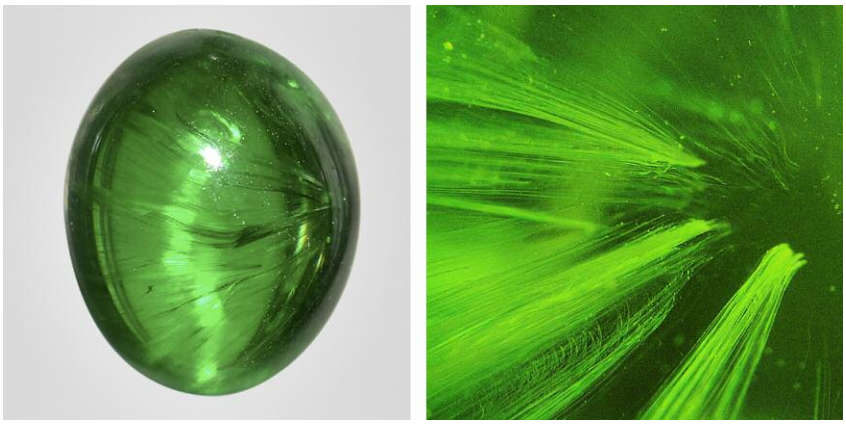

Figure 7. This 2.51 ct green demantoid with chatoyancy (left) contained well-aligned fibers of horsetail inclusions (right, field of view 1.10 mm).

GARNET

Cat's-Eye Demantoid and Brown Andradite with Horsetail Inclusions

Two garnets were recently submitted to the Tokyo lab for identification. One was a green cabochon weighing 2.51 ct; the other was an orangy brown round brilliant weighing 2.47 ct. Both had a refractive index (RI) over the limits of the refractometer and a hydrostatic specific gravity (SG) of 3.84. To confirm the identification, we used Raman spectroscopy. Both stones matched the andradite garnet group from the reference database. The ideal chemical formula of andradite is $Ca_3Fe_2Si_3O_{12}$. The most important feature in both garnets was their horsetail inclusions. The presence of horsetail inclusions, which are thought to consist of chrysotile fibers branching out and radiating toward the surface from a small chromite nodule, has been regarded as diagnostic for natural demantoid.

The 2.51 ct stone was a rare cat's-eye demantoid (figure 7). Demantoid garnet is by definition the green-colored andradite caused by chromium substitution. Chatoyancy is usually caused by closely spaced bands of long, thin parallel needles or fibers in the correct orientation, with a polished rounded surface such as a cabochon to reflect the light off the parallel inclusions. In this stone, the chatoyancy was due to the fibers of the horsetail inclusions. The radiating fibers were not parallel straight lines but parallel curves, so the "eye" was slightly curved.

The 2.47 ct stone was an andradite garnet with classic horsetails (figure 8). The dominant bodycolor was brown. The gemological properties and chemistry were classified as andradite in the garnet solid solution, but it was poorer in calcium and richer in iron and silicon than the ideal andradite composition. The brownish cast was due to

Figure 8. This 2.47 ct orangy brown andradite (left) contained radiating horsetail inclusions regarded as exclusive to demantoid (right, field of view 1.60 mm).

iron. On occasion we encounter stones with a strong yellow component that still have enough green to qualify as demantoid. However, this stone had no green in it and therefore was just andradite, not demantoid.

Consequently, the horsetail inclusions cannot be considered exclusively diagnostic for demantoid. They may also be found in non-green andradite. These two identifications—"cat's-eye demantoid" and normal "andradite" in spite of horsetail inclusions—were issued for the first time in GIA's colored stone report records.

Taku Okada and Philip G. York

Unusual Orange Pyrope-Spessartine-Grossular Garnet

GIA's New York laboratory recently examined an orange pear-shaped faceted stone (figure 9). Standard gemological testing revealed an RI of 1.771 and a hydrostatic SG of 3.89. The fluorescence reaction was inert to long-wave and short-wave UV light. The stone did not show any pleochroism when viewed with a dichroscope. Using a handheld spectroscope, absorption bands located at 410 and 430 nm in the blue and violet sections were clearly observed. All of these gemological properties are consistent with pyrope-spessartine garnet based on the classification system from Stockton and Manson ("A proposed new classification for gem-quality garnets," Winter 1985 *G&G*, pp. 205–218).

Besides standard gemological testing, all garnets submitted to GIA laboratories are routinely analyzed by energy-dispersive X-ray fluorescence (EDXRF) spectroscopy (see column 4 of the supplementary table available at https://www.gia.edu/gems-gemology/spring-2018-labnotes-unusual-orange-pyrope-spessartine-grossular-garnet). EDXRF results showed that the stone was predominantly composed of 15.37 mol.% pyrope, 53.70 mol.% spessartine, and—surprisingly—25.39 mol.% grossular. Unlike normal pyrope-spessartine garnet submitted to GIA that contains a small amount of grossular (less than 10 mol.%), this garnet had a much higher grossular component that had never been reported before in gem-quality garnets, to our knowledge. (Note that "malaia/malaya" is a trade name for yellowish, reddish, or pinkish orange pyrope-spessartine garnets that can potentially contain 2–94% spessartine, 0–83% pyrope, 2–78% almandine, 0–24% grossular, and 0–4% andradite. The garnet we examined falls into this concentration range.)

Figure 9. The unique composition of this 7.97 ct orange pear-shaped garnet was revealed as pyrope-spessartine-grossular.

To validate the accuracy of the chemistry, we performed laser ablation–inductively coupled plasma–mass spectrometry (LA-ICP-MS) analysis using a Thermo Fisher iCAP Qc ICP-MS coupled with a New Wave Research UP-213 laser ablation unit to obtain an additional set of chemical composition. USGS glass standard GSD-1G and GSE-1G were used as external standards. ^{29}Si was used as internal standard. The LA-ICP-MS results showed good agreement with the EDXRF results (see columns 1–3 of the supplementary table at https://www.gia.edu/gems-gemology/spring-2018-labnotes-unusual-orange-pyrope-spessartine-grossular-garnet).

Garnets are a group of isometric nesosilicates with the general chemical formula $X_3Y_2Z_3O_{12}$. Natural rock-forming silicate garnets are commonly divided into the pyralspite (pyrope, almandine, and spessartine) and ugrandite (uvarovite, grossular, and andradite) groups. In pyralspite, Al^{3+} occupies the Y-site and the X-site may contain Mg^{2+}, Fe^{2+}, or Mn^{2+}; these garnets are composed predominantly of pyrope ($Mg_3Al_2Si_3O_{12}$), almandine ($Fe^{2+}{}_3Al_2Si_3O_{12}$), and spessartine ($Mn_3Al_2Si_3O_{12}$) end members. Stockton and Manson (1985) presented a ternary plot (figure 10) to gemologically classify the pyralspite garnet species, and this showed the correlation among refractive index, visible spectroscopic observation, and chemistry. They determined that pyrope-spessartine should have an RI between 1.740 and 1.780 along with clear 410 and 430 nm absorption bands. We concluded that the orange pear-shaped garnet should be classified gemologically as pyrope-spessartine garnet.

To understand why this garnet with a high grossular component still shows the same gemological properties of normal pyrope-spessartine, we plotted the orange garnet chemistry in this ternary plot by combining pyrope with a grossular component. The orange spot representing the orange garnet appeared in the pyrope-spessartine region, because the refractive index of pure pyrope (1.714)

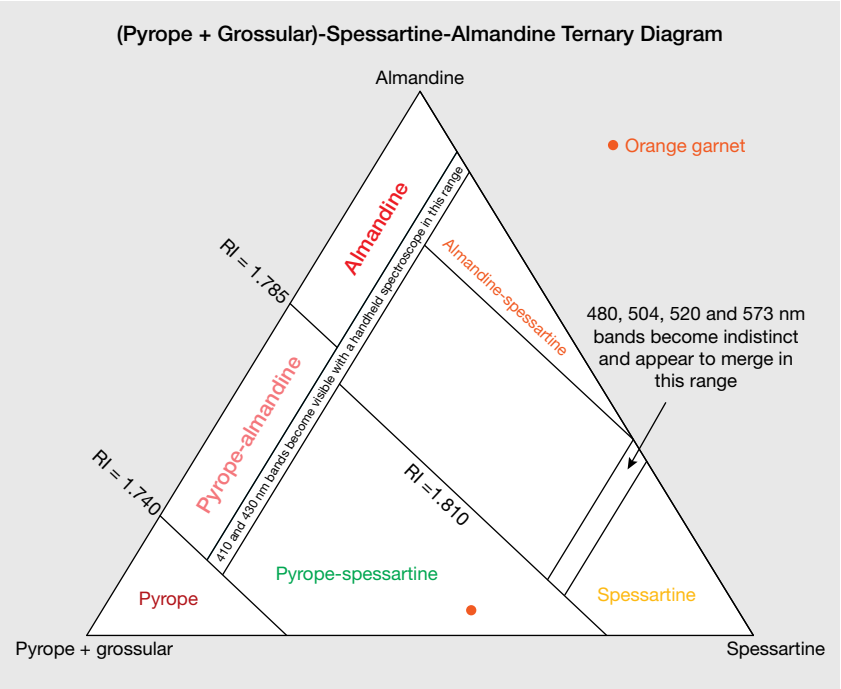

Figure 10. (Pyrope + grossular)-spessartine-almandine ternary diagram with data points based on molecular percentages for pyralspite garnet (modified after Stockton and Manson, 1985). The orange spot is the average of three sets of LA-ICP-MS data (table 1, columns 1–3). Refractive index and spectral boundaries are used to distinguish among the six proposed garnet species labeled in the diagram.

is close to and functions almost the same as the RI of pure grossular (1.734) in contributing to the combined refractive index. Since there is not a specific gemological species name for this orange garnet with higher grossular than pyrope component, the authors suggest that the stone be called *pyrope-spessartine-grossular*. This case demonstrates that sophisticated chemical analysis of garnet should be practiced routinely in gemological laboratories to make sure unique garnets are not misidentified.

Pamela Cevallos and Ziyin Sun

New Plastic IMITATION OPAL From Kyocera

Recently, the Carlsbad laboratory examined an interesting new gem material manufactured by the Japanese company Kyocera that displayed a play-of-color phenomenon. In the trade, this material may be sold as an "opal-like product," because of the play-of-color phenomenon observed (figure 11, left).

Standard gemological testing revealed a hydrostatic SG of 1.35. The refractive index was measured as 1.49. According to GIA, an imitation is defined as a natural or manmade material that mimics the appearance of, and is used as a substitute for, another gem material. Likewise, a synthetic gem is defined by GIA as a laboratory-grown gem material with virtually the same chemical and physical properties as a natural gem. Because the gemological properties for this new

Figure 11. This new plastic opal imitation (left) shows a very pleasing play-of-color that does not have the classic "snakeskin" columnar structure one would expect to see in traditional polymer-impregnated synthetic opal produced by Kyocera (right). The largest sample of plastic imitation opal in the left photo weighs 227 grams, and the largest sample of synthetic opal in the right photo weighs 65 grams. The rectangular black block in the photo on the left is 9.7 cm in length.

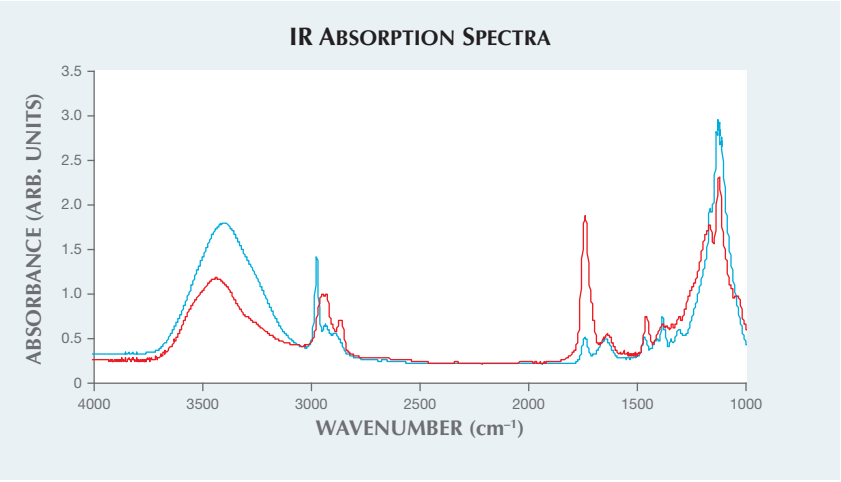

Figure 12. The infrared absorption spectrum of the new plastic imitation opal (red trace) was very similar to that of traditional plastic-impregnated synthetic opal (blue trace) except that the polymer feature at ~1734 cm^{-1} was about five times as strong.

Figure 14. Randomly oriented patches of play-of-color are uniformly distributed throughout this new plastic opal imitation. The imitation looks the same from all different angles. Field of view 13 mm.

material are out of range for natural opal (SG of 2.00 and RI between 1.37 and 1.47), it is best described as an imitation opal.

Further testing revealed that this material readily burns with a hot point and produces a strong acrid odor indicating that a significant amount of plastic is present. Additionally, advanced testing using EDXRF revealed the presence of silicon. Fourier-transform infrared (FTIR) testing revealed a spectrum that was quite similar to traditional polymer-impregnated synthetic opal (figure 11, right) except for a polymer peak that was nearly five times as strong (figure 12). These tests indicate that this material is composed of both plastic resin and silicon. When exposed to ultraviolet light, samples with a white bodycolor fluoresced a weak blue to short-wave and medium blue to long-wave UV. Samples with a black bodycolor fluoresced a weak orange to short-wave UV and were inert to long-wave UV.

Microscopic examination revealed some interesting features. The pattern in the play-of-color was random and unlike traditional synthetic opal did not display any "snakeskin" or "chicken wire" pattern (figure 13, left), but instead showed colored polygonal patches about 2 mm in size uniformly distributed throughout (figure 14). Nor did the plastic imitation opal display the columnar structure one would expect to see in synthetic opal (figure 13, right).

Visually, this new material is a very good imitation of natural opal. Gemologically, it is easy to separate from natural opal due to the comparatively high refractive index and low specific gravity. There are other pos-

Figure 13. Traditional synthetic opal shows a "chicken wire" or "snakeskin" pattern (left) and a columnar structure (right) that are diagnostic of synthetic origin. The new plastic opal imitation does not show these features. Fields of view 7.20 mm (left) and 14.40 mm (right).

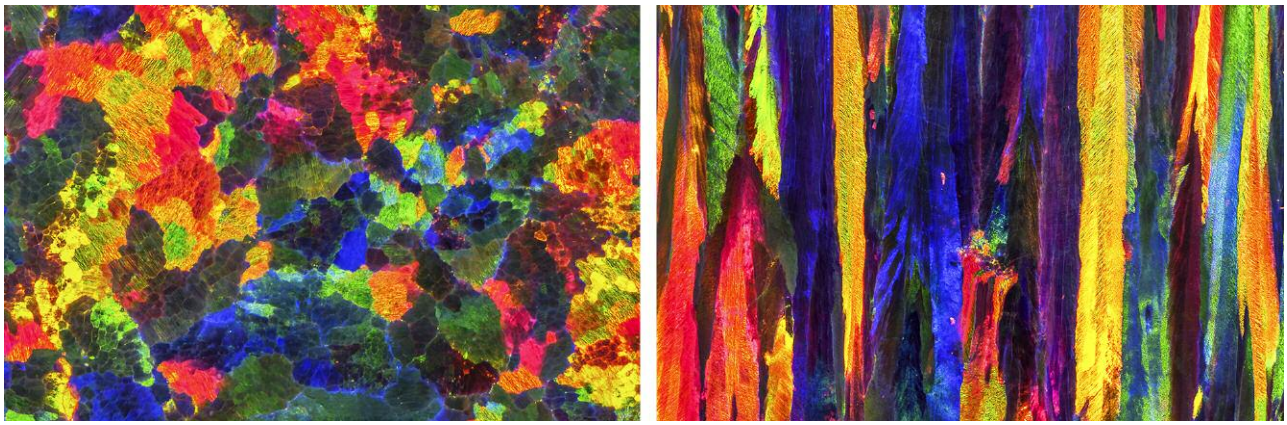

Figure 15. A natural blister that took the form of a pearlfish on the inner surface of one Pinctada maxima *valve. Courtesy of ECIJA.*

sible decorative applications for this plastic opal imitation material due to the large sizes that can be produced. This attractive material is a welcome addition to the gem trade and is easy to separate from natural opal with standard gemological testing.

Nathan Renfro and James E. Shigley

Natural Blister from Entombment of a Pearlfish Within a *Pinctada Maxima* SHELL

Pearlfish are marine fish of the Carapidae family that live symbiotically inside various invertebrate hosts. Occasionally, the remains of these fishes may be found completely covered by mother-of-pearl on the inner surfaces of some bivalve mollusks (J. Ballard, "The pearlfish," *African Wildlife*, Vol. 45, No. 1, 1991, pp. 16–19). The New York laboratory recently had the opportunity to examine a unique *Pinctada maxima* shell with a clear blister that took the form of a fish (figure 15). The shell dimensions were approximately 21 × 19 cm, and the entombed fish measured approximately 10 cm in length.

The *P. maxima* bivalve's soft internal body organs are enclosed and protected by the outer shell that is secreted by the mantle to form the beautiful inner nacreous mother-of-pearl layers and the pearls that are familiar to most (P.C. Southgate and J.S. Lucas, *The Pearl Oyster*, Elsevier, Oxford, UK, 2008, pp. 57–58). The hard surface of the oyster shell and the nooks within the shells provide places where a host of small animals such as pea crabs, shrimp, and fish can live. Pearl gemologists from GIA in Bangkok observed these within numerous *P. maxima* mollusks during a 2013 field expedition 80 miles off the coast of Broome, Western Australia. The shape and size of an example

Figure 16. An example of a living pearlfish with a slender, elongated shape and translucent body, found residing inside a P. maxima *shell during a 2013 GIA field expedition to Broome, Australia.*

recorded from the trip (figure 16) closely resembles the one examined by the lab.

There is a delicate harmony and balance between the mollusk and fish in their cohabitation. The pearlfish has been known to settle in the oyster shell for shelter and live in symbiosis without either one harming the other (E. Parmentier and P. Vandewalle, "Morphological adaptations of Pearlfish (Carapidae) to their various habitats," in A.L. Val and B.G. Kapoor, Eds., *Fish Adaptations*, Science Publishers, Enfield, New Hampshire, 2003, pp. 261–276). When the pearlfish eventually dies, the oyster cannot eject the organism and its self-healing mechanism

Figure 17. Microradiographic image of the pearlfish on the shell revealing the preserved details from head to tail beneath the nacre.

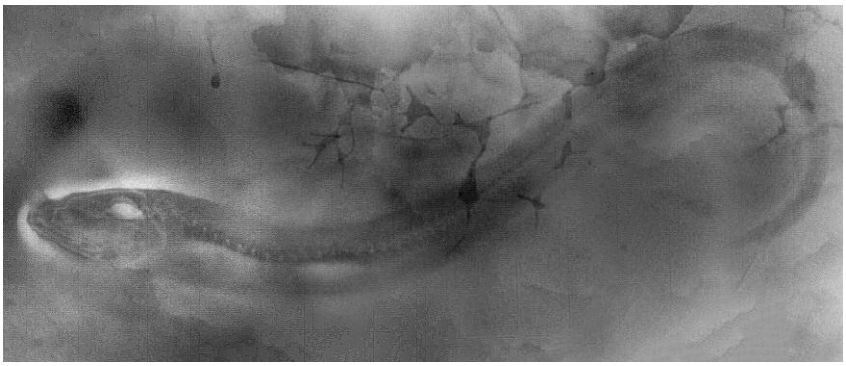

Figure 18. This 3.52 ct sample was the largest of a selection of recently submitted CVD synthetics.

kicks into action. The mollusk begins to deposit layers of nacre over the irritant to ease the likely discomfort experienced. The organism decomposes over time and the skeletal remains are left encased underneath the nacre to form a "blister" (GIA and CIBJO definition) on the inner surface of the shell.

The microradiographic images obtained for this sample examined by the New York laboratory show the fish's skeletal remains very clearly (figure 17). This extraordinary specimen is another prime example of Mother Nature's fascinating manifestations and was something out of the ordinary for everyone who handled and examined it in the laboratory.

Sally Chan and Emiko Yawaza

SYNTHETIC DIAMOND

Five CVD Synthetics Greater Than Three Carats

The quality and carat weight of CVD synthetic gem diamonds has increased dramatically over the last ten years (S. Eaton-Magaña and J.E. Shigley, "Observations on CVD-grown synthetic diamonds: A review," Fall 2016 *G&G*, pp. 222–245). Very recently a 6 ct round CVD synthetic was reported ("US lab creates 6ct. CVD synthetic," *Rapaport News*, Feb. 1, 2018). However, we still only occasionally receive CVD synthetic diamonds for grading reports, and very rarely do these submissions weigh more than three carats. In fact, GIA graded its first CVD synthetic over three carats not long ago, in October 2015 (Winter 2015 Lab Notes, pp. 437–439), and as of January 2018 had only examined a total of eight. So it was quite interesting when, in late January 2018, we received five CVD synthetics simultaneously (four known to be from the same client) that were all above three carats. The quality factors for these five samples submitted for synthetic diamond grading reports are presented in table 1, and the largest of the five is shown in figure 18.

TABLE 1. Summary of equivalent quality factors in five CVD synthetic diamonds.

Weight (ct)	Color	Clarity	Shape	Cut grade
3.02	F	VS_1	Cushion	n/a
3.12	G	VS_1	Round	Excellent
3.26	H	VS_2	Round	Excellent
3.37	H	VS_1	Cushion	n/a
3.52	J	SI_2	Round	Excellent

As table 1 shows, four of the five were in the near-colorless range and the smallest one was in the colorless range. Four had clarity grades equivalent to VS_1 or VS_2, while the largest was equivalent to SI_2. All three round brilliants received Excellent cut grades. These results are consistent with a recent survey (Eaton-Magaña and Shigley, 2016), which found that a majority of D-to-Z CVD synthetics are in the near-colorless range (67%) and that a slight majority have clarity grades equivalent to VVS_2–VS_1.

In keeping with standard GIA procedure, we performed IR absorption and PL spectroscopy on all five samples. As expected for CVD synthetics, all were identified as type IIa, showed pronounced silicon-related peaks in their PL spectra, and displayed striations in DiamondView imaging that are characteristic for CVD synthetics. All except the 3.52 ct sample also showed nickel-related peaks at 883/884 nm in their PL spectra with 830 nm excitation. We expect that submissions of CVD synthetics in this weight range and beyond will become more common in the next few years.

Sally Eaton-Magaña

Fancy Deep Brown-Orange CVD Synthetic Diamond

A 0.56 ct diamond (figure 19) was color graded as Fancy Deep brown-orange. The diamond was found to be a CVD-grown synthetic that had been irradiated and annealed, perhaps multiple times. DiamondView imaging (figure 20) showed the telltale striations of the CVD growth process, and the PL spectrum showed the SiV^- (736/737 nm doublet) commonly found in CVD synthetics. The Vis-NIR spectrum (figure 21) showed a GR1 defect (the neu-

Figure 19. A face-up image showing the deep brown-orange bodycolor of a CVD-grown synthetic that has been irradiated and annealed.

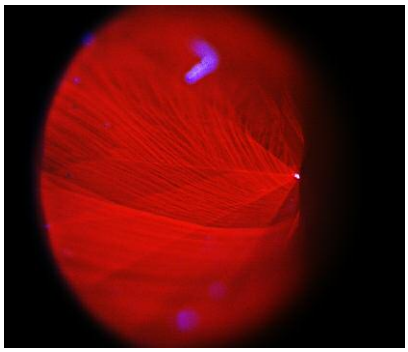

Figure 20. A DiamondView image reveals the characteristic growth striations of a CVD-grown synthetic diamond.

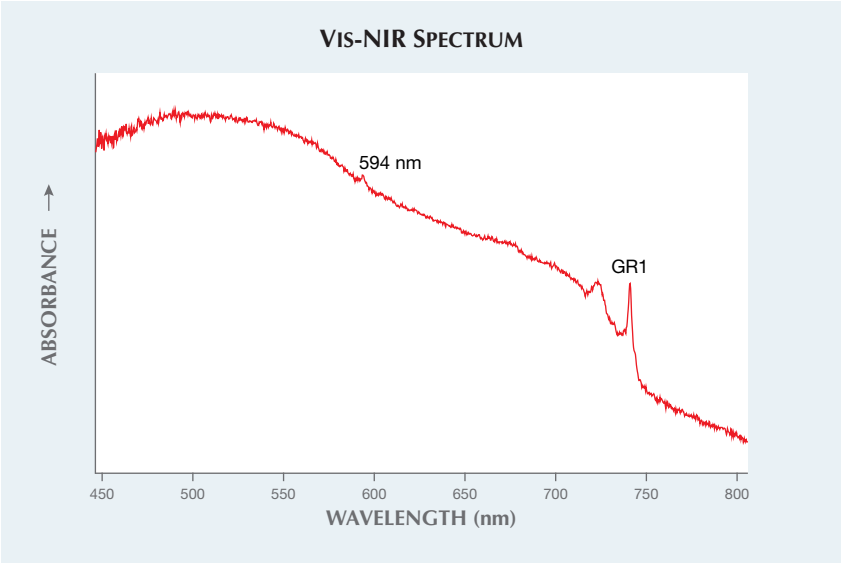

Figure 21. The visible-NIR spectrum of the irradiated and annealed CVD synthetic shows the GR1 and 594 nm defects.

tral vacancy center) and a peak at 594 nm that is commonly seen in diamonds that have been irradiated and annealed. This is in contrast to the normal irradiated and annealed CVD synthetic diamonds that show features related to nitrogen vacancies. The PL spectrum shows the NV^0 (575 nm) and NV^- (637 nm) peaks in relatively high concentrations compared to the diamond Raman line. In the infrared spectrum, a clear band at 1130 cm^{-1} and a peak at 1344 cm^{-1} indicate the presence of single substitutional nitrogen.

CVD-grown synthetic diamonds have been known to be irradiated (Fall 2014 Lab Notes, pp. 240–241; Fall 2015 Lab Notes, pp. 320–321) and also irradiated and annealed (J. Shigley et al., "Lab-grown colored diamonds from Chatham Created Gems," Summer 2004 *G&G*, pp. 128–145). The irradiation and annealing performed on CVD synthetics is generally done on those with isolated nitrogen and produces a pink to red bodycolor. This color is caused by nitrogen-vacancy centers created when the vacancies produced by irradiation combine with the isolated nitrogen during the annealing process. In this case, the diamond showed a brown-orange bodycolor due to the combination of the isolated nitrogen and irradiation features. The stone in question contained isolated nitrogen, so it is possible that the intent was to create a pink to red color, but the treatment did not produce the expected results. Brown-orange color as a result of treatment has not been seen in a CVD synthetic diamond before, so the intentions of the treatment are as yet unknown.

Troy Ardon and Nicole Ahline

PHOTO CREDITS
John I. Koivula—1, 2; Robison McMurtry—3, 9, 18, 19; Nathan Renfro—4, 5, 13, 14; Tony Leung—6 (left); Billie Law—6 (right); Shunsuke Nagai—7 (left), 8 (left); Taku Okada—7 (right), 8 (right); Diego Sanchez—9; Robert Weldon—11; Jian Xin (Jae) Liao—15, 17; Areeya Manustrong—16; Nicole Ahline—20.